Int J Thermophys (2009) 30:265–275
DOI 10.1007/s10765-008-0438-5

In situ Gas Temperature Measurements by UV-Absorption Spectroscopy

A. Fateev · S. Clausen

Abstract The absorption spectrum of the NO $A^2\Sigma^+ \leftarrow X^2\Pi\,\gamma$-system can be used for in situ evaluation of gas temperature. Experiments were performed with a newly developed atmospheric-pressure high-temperature flow gas cell at highly uniform and stable gas temperatures over a 0.533 m path in the range from 23 °C to 1,500 °C. The gas temperature was evaluated (1) from the analysis of the structure of selected NO high-resolution γ-absorption bands and (2) from the analysis of vibrational distribution in the NO γ-absorption system in the (211–238) nm spectral range. The accuracy of both methods is discussed. Validation of the classical Lambert–Beer law has been demonstrated at NO concentrations up to 500 ppm and gas temperatures up to 1,500 °C over an optical absorption path length of 0.533 m.

Keywords High gas temperature · Nitric oxide · Lambert–Beer law · UV absorption spectroscopy · Vibrational relaxation

1 Introduction

In situ simultaneous high-speed measurements of gas temperature and gas composition are an important task for many industrial processes. In many cases, the measurements have to be done in a very aggressive and unstable (in time) hot gas environment as realized, for example, in combustors and engines. Typically, the temperature range of interest for in situ diagnostics of hot gases varies from 500 °C to 1,500 °C. An optically based technique is beneficial because it is non-intrusive, accurate, has a short response time, and can be performed in situ under various extremely hazardous conditions.

A. Fateev (✉) · S. Clausen
Risø National Laboratory for Sustainable Energy, Technical University of Denmark - DTU,
Frederiksborgvej 399, 4000 Roskilde, Denmark
e-mail: alexander.fateev@risoe.dk

Infrared (IR)-based in situ optical diagnostics of hot gases have been extensively developed for many years in our lab and have been successfully used in practice at various industrial sites in Denmark and Europe. In very humid and hot environments, ultraviolet (UV) techniques are more sensitive for measurements of, for example, NO. In our present work, we have extended in situ optically based diagnostics to the UV range in order to evaluate gas temperature from the analysis of UV-absorption spectra. The development of methods for gas concentration measurements requires that the gas temperature is known or measured.

2 Experimental Setup

Measurements have been performed on our newly developed atmospheric-pressure high-temperature flow gas cell (HGC), Fig. 1. The gas cell was designed as a flow gas cell with a so-called laminar window, nozzle seal cell principle, but with care to obtain a similar uniform gas temperature profile and well-defined path length as for the other two gas cells with hot windows in our laboratory.

The HGC consists of three different parts: a high-temperature sample cell with a length of 0.533 m and two "buffer" cold gas parts on the left and right sides of the hot sample cell. The buffer parts are filled with a UV/IR-transparent (purge) gas (e.g., N_2), whereas the central sample cell can be filled with the gas under investigation (e.g., $N_2 + NO$). The aperture of the sample cell is kept small (i.e., diameter of 15 mm) in order to reduce heat transfer by radiation from the sample cell and to reduce the risk of collapse of well-defined flows in the laminar windows. The laminar windows also function as radiation shields. Similarly, apertures placed at the end parts between the laminar windows and the cold windows reduce the heat losses by radiation and convection by breaking down the vortices created by the thermal gradient in the buffer sections. High-quality pure ceramics were used in order to minimize hetero-phase reactions and to avoid contact of the sample gas with any hot metal parts. A uniform temperature profile is obtained by heating the gas cell with a dedicated three-zone furnace in order to compensate the heat loss at the ends of the gas cell. The sample gas is preheated. Flows of the gases in the sample cell and in the buffer parts are kept at about the same flow rates. The outer windows placed on the ends of the buffer parts are replaceable. In all experiments, KBr windows have been used. The gas flow through

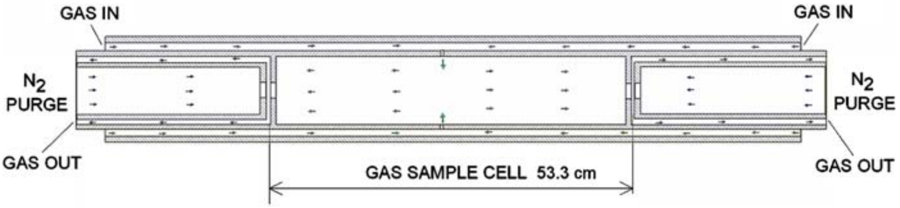

Fig. 1 High-temperature flow gas cell (HGC) used in the experiments. Arrows show directions of the gas flows

the HGC maintains a highly uniform and stable temperature in the range from 23 °C to 1,500 °C.

The HGC performance has been carefully tested by flow visualization calculations and by IR emission/absorption measurements for various temperatures in the sample cell and various gas flows in the sample cell and in the buffer parts. Further details of the experimental set up will be presented and discussed in another paper [1].

High-resolution UV-absorption measurements were performed with a 0.5 m UV/VIS-spectrometer (Acton Research) equipped with a UV-optimized holographic grating ($1200\,\mathrm{grooves}\cdot\mathrm{mm}^{-1}$) and a UV-enhanced PIXIS CCD-camera with 1340 × 100 pixels (Princeton Instruments). The dispersion of the grating was sufficient to observe a range of 28 nm on the CCD, allowing simultaneous recording (without the movement of the grating) of three UV γ-absorption bands of NO ($A^2\Sigma^+ \leftarrow X^2\Pi$): $A,v' = 1 \leftarrow X,v'' = 0$, $A,v' = 0 \leftarrow X,v'' = 0$, and $A,v' = 0 \leftarrow X,v'' = 1$. A spectral resolution of $\Delta\lambda = 0.048$ nm for all UV-absorption measurements with the 0.5 m UV/VIS spectrometer was achieved with an entrance slit width of 20 µm.

A highly stable deuterium lamp (Oriel Instruments) with a UV-condenser was utilized as a parallel-beam light source in the range from 190 nm to 400 nm. The UV-light beam, after passing through the HGC, was focused by means of a short-focal-length CaF_2 lens into a 0.5 m long fused-silica optical fiber coupled to the entrance slit of the UV/VIS spectrometer. The uncorrected spectrum of the deuterium lamp/fiber combination over (190–400) nm presents continuum-like behavior with a broad maximum at (240–250) nm decreasing to zero at around 180 nm, due to the transmission limitations of the CaF_2 lens, the optical fiber, and the diminishing sensitivity of the spectrometer + CCD system.

In the experiments, mixtures of $N_2 + NO$ (100 ppm to 1,000 ppm) and $N_2 + O_2$ (4.5 %) + NO (200 ppm to 500 ppm) at a flow rate of about $2\,L_n\cdot\mathrm{min}^{-1}$ have been used. Calibrated mass-flow controllers were used to control the gas flows. Different NO concentrations were obtained by flow mixing of N_2 and $N_2 + NO$ (1 %) gases at different $N_2 : N_2 + NO$ (1 %) ratios. UV-absorption measurements were performed at four different temperatures: 23 °C, 500 °C, 1,000 °C, and 1,500 °C.

The gas temperature and the temperature uniformity along the axis of the high-temperature central part of the HGC were verified by thermocouple measurements at three different points inside the HGC and by IR-emission/absorption measurements of the $N_2 + CO_2$ (1 %) gas mixture [2] in a separate set of measurements preceding the NO absorption experiments. The temperature uniformity over 0.45 m was found to be better than ±1 °C, or on average, ±0.5 °C.

3 Absorption Spectra Analysis

Absorption and emission spectra of the NO $A^2\Sigma^+ \leftarrow X^2\Pi\gamma$-system measured with high spectral resolution shows complicated structure corresponding to a variety of rovibronic transitions, v', $J' \leftarrow v''$, J'', between different electronic states A and X of NO. The intensity of each rovibronic transition can be characterized by an integrated Einstein absorption coefficient, $B_{j'j''}$ which can be calculated from the Einstein emission coefficient, $A_{v'v''}$ for the associated vibronic transition, $v' \leftarrow v''$, available in the literature [3]. The method is described in detail in, for example, the work of Reisel et al. [4].

Calculation of a "*true*" absorption spectrum for a vibronic band, $v' \leftarrow v''$, needs knowledge about (1) the $B_{j'j'}$ coefficients, (2) the line shape function of rovibronic transitions, which in the case of atmospheric-pressure hot gases can be assumed to be a Voigt function, and (3) the distribution over rotational levels. In most cases, a Boltzmann distribution over rotational levels $N_{J''}$ with rotational temperature T_{rot} can be used. Since rotational relaxation (*R*–*T* process) takes place in a very short time scale ($\tau_{\text{rot}} \sim 20\,\text{ns}$) corresponding to 3–10 collisions under normal conditions for molecules like N_2, O_2, and NO, T_{rot} will always equal the gas temperature, T. A full *true* absorption spectrum can be calculated based on a set of $A_{v'v''}$ for various $v' \leftarrow v''$ bands and assuming some distribution over vibronic states in the ground state. The latter is often taken as a Boltzmann distribution $N_{v''}$ with vibrational temperature T_{vib}. The time needed for vibrational relaxation, τ_{vib}, (*V*–*T* process) is significantly longer than τ_{rot} and can extend up to 1 ms or even 0.1 s [5,6]. At thermodynamic equilibrium, T_{vib} will always be equal to T.

A "*real*" absorption spectrum corresponding to light absorption in a gas slab governed by the classical Lambert–Beer law can be calculated by taking into account the concentration of absorbing species, knowledge of the optical path length, and the instrumental line-shape function. In many practical cases, the FWHM (full width at half maximum) of the instrumental line shape is significantly greater than the Voigt profile FWHM and a *real* spectrum will mostly depend on the instrumental line-shape function. Thus, for example, the Voigt profile FWHM calculated for NO A,$v' = 1 \leftarrow$ X,$v'' = 0$ ($\lambda = 215\,\text{nm}$), taking into account Doppler and pressure broadening, will be $\Delta\lambda^{\text{Voigt}} = 0.0038\,\text{nm}$ and $\Delta\lambda^{\text{Voigt}} = 0.0027\,\text{nm}$ at 23 °C and 1,000 °C, respectively [7]. In these cases, the *real* spectrum will be mainly determined by the instrumental line-shape function. A useful example calculation of the *real* NO $A^2\Sigma^+ \leftarrow X^2\Pi\gamma$-system absorption spectra for $\Delta v = 0, 1$, incorporating Doppler and pressure broadening effects at different pressures (up to 3.5 bar) and temperatures (up to 1,490 °C), is represented in the recent paper by Trad et al. [8].

In the present work, we used our own program and LIFBASE software [9] to calculate the absorption spectra in "*arbitrary units*" for chosen NO vibronic transitions: A,$v' = 1 \leftarrow$ X,$v'' = 0$ ($\lambda = 215\,\text{nm}$), A,$v' = 0, 1 \leftarrow$ X,$v'' = 0, 1$ ($\lambda = 224, 226\,\text{nm}$), and A,$v' = 0 \leftarrow$ X,$v'' = 1$ ($\lambda = 236\,\text{nm}$). The NO absorption spectrum in *arbitrary units* was calculated from the *true* absorption spectrum convolved with the instrumental line-shape function. Calculated spectra at various T_{rot} were compared with, and scaled to, an experimental absorption spectrum, taking into account the accuracy of the experimental data in order to minimize discrepancies between the experimental and calculated spectra in the wavelength scale and in the integral value scale (the integral value is obtained through integration over the vibronic band). Since $T = T_{\text{rot}}$, the best fit to the experimental absorption spectrum gives us the value of the gas temperature in the HGC.

Only Doppler broadening was taken into account since the instrumental line-shape function FWHM evaluated from the Hg-emission line ($\lambda = 297\,\text{nm}$) of a standard Hg lamp and corrected to the spectrometer dispersion in the range of (211–238) nm was nearly constant at $\Delta\lambda = 0.048\,\text{nm}$, a value that is 17 times higher than the Voigt profile FWHM at 1,000 °C. Nevertheless, to prove it, an absorption spectrum $\mathrm{A},v' = 1 \leftarrow \mathrm{X},v'' = 0$ ($\lambda = 215\,\mathrm{nm}$) at $T_{\mathrm{rot}} = 1{,}000\,°\mathrm{C}$ with an instrumental FWHM of $\Delta\lambda = 0.018\,\mathrm{nm}$ and artificial Doppler profile FWHM of $\Delta\lambda^{\mathrm{Doppler}} = 0.0027\,\mathrm{nm}$ (used as an approximation of the Voigt profile FWHM at 1,000 °C) was calculated and compared with the spectrum calculated with $\Delta\lambda^{\mathrm{Doppler}} = 0.001\,\mathrm{nm}$ (Doppler profile FWHM at 1,000 °C) and the same instrumental FWHM. Only a very small difference in the two calculated spectra was found.

As is well known, deviation from the Lambert–Beer law frequently appears if the instrumental spectral resolution is too low compared with the absorption line width [9]. As was mathematically demonstrated in [10], the instrument resolution influences the apparent optical depth (a product of the absorption cross section, species concentration, and absorption path length). In general, the instrumental spectral resolution (FWHM) should be less than one-fifth of the absorption linewidth in order to obtain the true value of the optical depth [9]. In order to investigate the influence of instrument resolution on the measured NO absorption spectra, we calculated "apparent" optical depths at various instrumental resolution values for $T = 500\,°\mathrm{C}$. Indeed, the spectral shape of the "apparent" optical depth depends on the value of the instrumental resolution, as pointed out in [10]; the maximum of a rotational line becomes lower but the width of the line (FWHM) increases. Only when the instrumental resolution is significantly less (by more than five times) than the true absorption line width (determined by the Voigt function) does the spectral shape of the "apparent" optical depth achieve its true value. However, the integral values of the "apparent" optical depths, $\int_{\mathrm{band}} \ln\left(\frac{I_0(\lambda)}{I(\lambda)}\right) \mathrm{d}\lambda$, used in our work (see below) do not depend on the instrumental resolution and they are equal to the integral value of the "true" optical depth, and are only determined by Doppler and Lorentz broadenings. In all calculations, the collisional broadening parameters summarized in [8] were used.

4 Results

4.1 Validation of Lambert–Beer Law

Simple calculations based on $B_{j'j''}$ values from [11] show that, at 1,500 °C and for an optical path length of 0.533 m, saturation for a single v', $J' \leftarrow v''$, J' line in a *true* absorption spectrum appears at an NO concentration of 100 ppm, assuming an instrumental line FWHM equal to the Doppler-profile FWHM with $\Delta\lambda^{\mathrm{Doppler}} = 0.0027\,\mathrm{nm}$ and $B_{j'j''} = 3.4 \times 10^{17}\,\mathrm{m}^3 \cdot \mathrm{J}^{-1} \cdot \mathrm{s}^{-2}$. However, the true Voigt line-shape function with the same FWHM will give a higher threshold for NO absorption saturation because of its Lorentz wings. Nevertheless, if the NO concentration is more than 100 ppm and $\Delta\lambda \gg \Delta\lambda^{\mathrm{Voigt}}$, validation of the Lambert–Beer Law is needed.

In Fig. 2, NO absorption spectra at various gas temperatures and an NO concentration of 390 ppm are shown. The intensity of the $\mathrm{A},v' = 0 \leftarrow \mathrm{X},v'' = 1$ ($\lambda = 236\,\mathrm{nm}$) absorption band follows the temperature rise. In Fig. 3, integrated values (balls), $\int_{\mathrm{band}} \ln\left(\frac{I_0(\lambda)}{I(\lambda)}\right) \mathrm{d}\lambda$, of the NO $\mathrm{A},v' = 1 \leftarrow \mathrm{X},v'' = 0$ ($\lambda = 215\,\mathrm{nm}$) absorption band calculated at different NO concentrations and $T = 500\,°\mathrm{C}$ are shown. The reference spectrum, I_0 (λ), was measured with N_2 (99.998 %) flowing through the

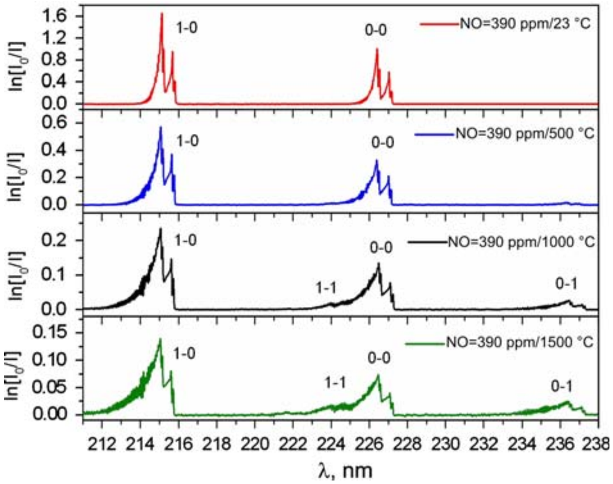

Fig. 2 NO $A^2\Sigma^+ \leftarrow X^2\Pi$ γ-system absorption spectra in the range of (211–238) nm measured at [NO] = 390 ppm and various temperatures: 23 °C, 500 °C, 1,000 °C, and 1,500 °C. Spectral resolution is 0.048 nm

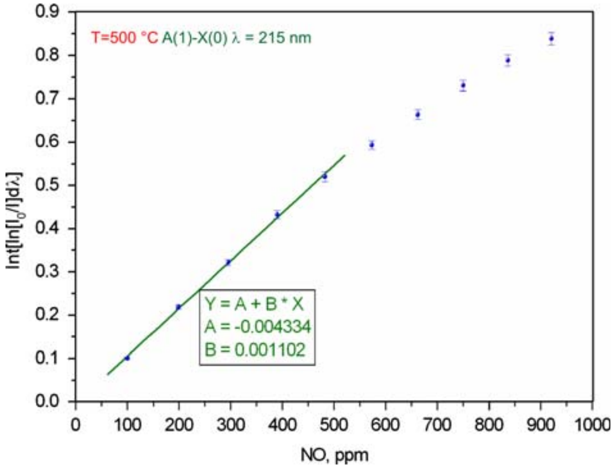

Fig. 3 Integrated values of the NO $A, v' = 1 \leftarrow X, v'' = 0$ ($\lambda = 215$ nm) absorption band at various NO concentrations. Uncertainties in the measurements (around 2 %) are shown as vertical bars. The gas temperature is 500 °C

gas cell. During the measurements, the flow rates of N_2 and N_2 + NO (100 ppm to 1,000 ppm) were kept at about $2\,L_n \cdot min^{-1}$ in order to maintain the temperature uniformity. Regions of linear and nonlinear NO absorption are clearly seen. Thus, at NO concentrations of (0–500) ppm, the experimental points can be fitted by a linear function that crosses the origin very close to zero (Fig. 3). At NO concentrations greater than 500 ppm, saturation effects become significant.

The same dependences were observed at 23 °C, 1,000 °C, and 1,500 °C. For the following analysis, only the first four or five points in the range of NO concentrations

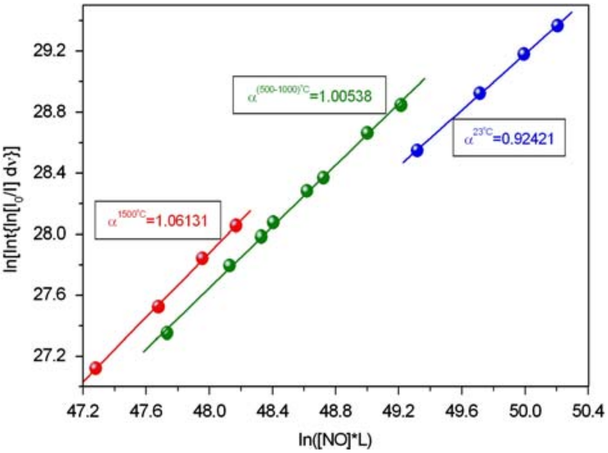

Fig. 4 Validation of the Lambert–Beer law. Values of α associated with different T are shown close to the fit lines

from 100 ppm to 500 ppm were selected at all temperatures. It should be also noted that all fits over the first four or five points drawn through the graph origin indicate linear behavior in NO absorption.

Deviations from the Lambert–Beer law were considered by Donovan et al. [12], who proposed a modified form of the law by introducing a new parameter, α:

$$\ln\left(\frac{I_0(\upsilon)}{I(\upsilon)}\right) = (\sigma(\upsilon)L[\mathrm{X}])^{\alpha}\,, \tag{1}$$

where $I_0(\upsilon)$ and $I(\upsilon)$ are reference and detected light intensities, respectively; [X] is the species concentration, e.g., X = NO; L is the absorption optical path length; $\sigma(\upsilon)$ is the absorption cross section; and υ is the frequency.

However, it was shown in the literature that this form will only be valid for a limited range of the product $[\mathrm{X}]L$ where the coefficient α remains constant [12]. Following Trad et al. [8], Eq. 1, with small modification, can be rewritten as

$$\ln\left[\int_{\text{band}} \ln\left(\frac{I_0(\upsilon)}{I(\upsilon)}\right)\mathrm{d}\upsilon\right] = \alpha\ln([\mathrm{X}]L) + \ln\int_{\text{band}} \sigma(\upsilon)^{\alpha}\mathrm{d}\upsilon, \tag{2}$$

In Fig. 4, the left side of Eq. 2 is plotted versus $\ln([\mathrm{X}]L)$ for various temperatures and NO concentrations. Measurements at 500 °C and 1,000 °C can be perfectly fitted by one line with a value of α very close to unity, 1.005 ± 0.015. The fit for 1,500 °C gives a slightly higher value, 1.061 ± 0.018. On the contrary, the fit for 23 °C shows a value less than unity, 0.924 ± 0.011. Recalling the earlier discussion in connection with Fig. 3, we conclude that the classical Lambert–Beer law is valid for temperatures from 500 °C to 1,500 °C; therefore, the gas temperature can be directly evaluated (without any spectral corrections) from the NO vibronic absorption spectra.

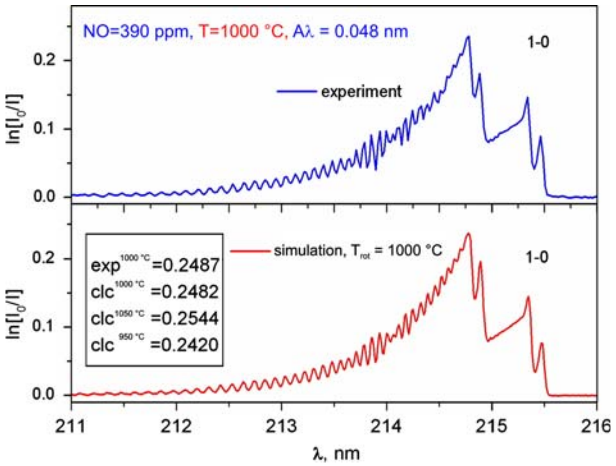

Fig. 5 Experimental absorption spectrum (*top panel*) and calculated one (*bottom panel*) for [NO] = 390 ppm and $T_{\mathrm{rot}} = 1{,}000\,°\mathrm{C}$. The gas temperature is 1,000 °C. The spectral resolution is $\Delta\lambda = 0.048$ nm

4.2 Gas Temperature Evaluation from the 1–0 Absorption Band

Absorption spectra measured at temperatures from 500 °C to 1,500 °C and NO concentrations less than 500 ppm have been used to evaluate the gas temperature. A typical absorption spectrum at 1,000 °C for an NO concentration of 390 ppm and its simulation are shown in Fig. 5. Very good agreement of the calculated ($T_{\mathrm{rot}} = 1{,}000\,°\mathrm{C}$) and measured spectra is observed, and particularly good agreement is obtained for the integral values, $\int_{\mathrm{band}} \ln \frac{I_0(\lambda)}{I(\lambda)} \mathrm{d}\lambda$; the integral values for the experimental and calculated spectra in Fig. 5 are 0.2487 and 0.2482, respectively. The sensitivity of the gas temperature evaluation for $\Delta T = \pm 50\,°\mathrm{C}$ was estimated by calculating several spectra at different rotational temperatures, e.g., 950 °C, 1,000 °C, and 1,050 °C, and comparing them with the experimental spectrum in terms of wavelength and integral value, taking into account the accuracy of the experimental data. The integral values for the spectra calculated at 950 °C and 1,050 °C are 0.2420 and 0.2544, respectively. The sensitivity remains the same for $500\,°\mathrm{C} < T < 1{,}500\,°\mathrm{C}$.

4.3 T_{vib} Evaluation from NO Absorption Spectrum

If the temperature of the gas increases, vibronic levels different from $\nu'' = 0$ will be populated and $N_{\upsilon''}$ can be described by a Boltzmann distribution:

$$N_{\upsilon''} \propto \mathrm{e}^{-\frac{E_{\upsilon''}}{kT_{\mathrm{vib}}}}, \tag{3}$$

where $E_{\upsilon''}$ is the energy of vibronic state ν''.

$E_{\upsilon''}$ can be calculated from the known spectroscopic constants of NO(X) [13]. $N_{\upsilon''}$ is related to the Lambert–Beer law for linear absorption, Eq. 1. Since $\int_{\mathrm{band}} \sigma(\upsilon)\mathrm{d}\upsilon \propto B_{\upsilon'\upsilon''} h\upsilon_{\upsilon'\upsilon''}$, Eq. 3 can be rewritten as

Table 1 Summary of calculations of the T_{vib} for $\upsilon'' = 0, 1$ obtained from NO absorption spectra in different gas mixtures measured in the range from 211 nm to 238 nm and at gas temperatures of 500 °C, 1,000 °C, and 1,500 °C

Gas mixture	T_{vib} (°C)		
	$T = 500\,°\text{C}$	$T = 1{,}000\,°\text{C}$	$T = 1{,}500\,°\text{C}$
$N_2 + NO$ (100–500 ppm)	596 ± 36	1093 ± 65	1500 ± 42
$N_2 + O_2$ (4.5 %) + NO (100–500 ppm)	580 ± 40	1060 ± 68	1630 ± 45

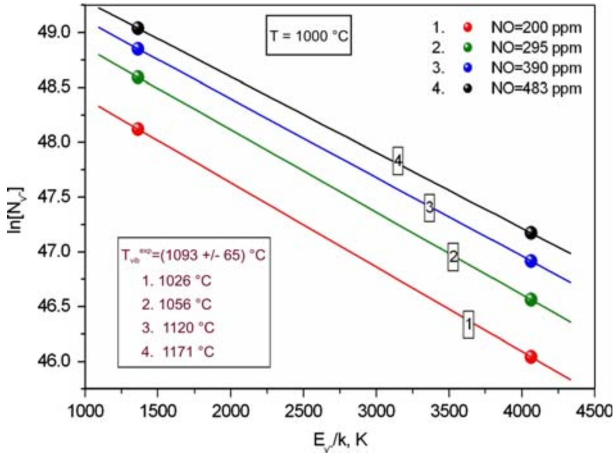

Fig. 6 Evaluation of T_{vib} from the NO absorption spectra at $T = 1{,}000\,°\text{C}$ and various NO concentrations: 200 ppm, 295 ppm, 390 ppm, and 483 ppm. The average temperature is $T_{\text{vib}} = (1{,}093 \pm 65)\,°\text{C}$

$$\ln\left[\frac{1}{L \cdot B_{\upsilon'\upsilon''}} \int_{\text{band}} \ln\left(\frac{I_0(\upsilon)}{I(\upsilon)}\right) \mathrm{d}\upsilon\right] \propto -\frac{E_{\upsilon''}}{kT_{\text{vib}}}. \tag{4}$$

From the slope of the line in the coordinates of the left side of Eq. 4 and $E_{\upsilon''}/k$, the value of T_{vib} can be calculated. Therefore, the vibrational temperature can be evaluated from a broad absorption spectrum taking into account at least two vibronic bands corresponding to different values of υ''. An example of a T_{vib} calculation at $T = 1{,}000\,°\text{C}$ and various NO concentrations is shown in Fig. 6 for $\upsilon'' = 0, 1$. The calculated T_{vib} values for $500\,°\text{C} < T < 1{,}500\,°\text{C}$ and various NO concentrations (100 ppm to 500 ppm) are summarized in Table 1. Each temperature is an average of four or two measurements at different NO concentrations in N_2 + NO and N_2O_2 (4.5 %) + NO gas mixtures, respectively.

As can be seen from Table 1, T_{vib} calculated from NO vibronic absorption bands in the N_2 + NO mixture differs by approximately 100 °C from the corresponding gas temperatures of 500 °C or 1,000 °C but fits a temperature of 1,500 °C. Since the Lambert–Beer law, Eq. 1, is valid (Sect. 4.1) for $500\,°\text{C} < T < 1{,}500\,°\text{C}$ and NO concentrations less than 500 ppm, such a good fit at 1,500 °C cannot be explained only by the absorption effect due to a lower gas density at 1,500 °C compared to that at 500 °C or 1,000 °C. Moreover, the observed difference between T_{vib} and T from 500 °C to 1,000 °C should also be seen at 1,500 °C. Indeed, due to the population of rovibronic levels with $55 < J'' < 60$ at $T = 1{,}500\,^{\circ}\mathrm{C}$, the energies of these levels for $N_2(X,v'' = 1)$ and NO $(X,v'' = 2)$ become close to each other and therefore the probability of resonance $V - V'$ energy exchange will increase. This will probably lead to continuous "pumping" of the NO $(X,v'' = 2)$ level followed by V–T relaxation to the NO(X,v'') manifold. As a result, T_{vib} becomes slightly higher than T. The same explanation can also be applied in order to understand the 130 °C difference between T_{vib} and T in the $N_2 + O_2$ (4.5 %)+NO mixtures at 1,500 °C. Again, at 1,500 °C, the rovibronic levels of O_2 $(v'' = 3)$ and NO $(X,v'' = 2)$ are close to each other for $45 < J'' < 57$. Moreover, the relative population of rovibronic levels of $O_2(v'' = 3, J'')$ and NO $(X,v'' = 2, J'')$ at $45 < J'' < 57$ is higher compared to the same one for $N_2(X,v'' = 1)$ and NO $(X,v'' = 2)$ at $55 < J'' < 60$. That probably causes the difference of 130 °C in T_{vib} and T in the $N_2 + O_2$ (4.5 %) + NO mixture at 1,500 °C compared to the 0 °C difference in the case of $N_2 +$ NO, Table 1.

5 Conclusions

In our work, we have demonstrated that the absorption spectrum of the NO $A^2\Sigma^+ \leftarrow X^2\Pi\gamma$-system can be used for in situ evaluation of gas temperature for NO concentrations up to 500 ppm and gas temperatures up to 1,500 °C for an optical absorption path length of 0.533 m. The validation of the classical Lambert–Beer law has been demonstrated. The gas temperature can be evaluated from the analysis of a single NO vibronic absorption band or from the entire broad absorption spectrum in the range from 211 to 238 nm. The sensitivity of T evaluated from the rovibronic distribution in the NO $A,v' = 1 \leftarrow X,v'' = 0\,(\lambda = 215\,\mathrm{nm})$ absorption band is $\Delta T = \pm 50\,^{\circ}\mathrm{C}$, whereas analysis of the broad absorption spectrum gives $T = T_{\mathrm{vib}} - 100\,^{\circ}\mathrm{C}$ with $\Delta T_{\mathrm{vib}} = \pm\,(30\text{–}70)\,^{\circ}\mathrm{C}$ in the range from 500 °C to 1,000 °C. Quasi-resonance V–V' collisions with N_2 and O_2 probably result in a slightly "heated" NO(X,v'') vibronic distribution. However, further investigation is needed.

Acknowledgment This work was supported by Energinet.dk Project No. 2006 1 6382.

References

1. S. Clausen, K.A. Nielsen, A. Fateev, to be submitted to Meas. Sci. Technol
2. J. Bak, S. Clausen, J. Quant. Spectrosc. Radiat. Transfer **61**, 687 (1999)
3. L.G. Piper, L.M. Cowles, J. Chem. Phys. **85**, 2419 (1986)
4. J.R. Reisel, C.D. Carter, N.M. Laurendeau, J. Quant. Spectrosc. Radiat. Transfer **47**, 43 (1992)
5. R.C. Millikan, D.R. White, J. Chem. Phys. **39**, 3209 (1963)
6. A. Lifshitz, J. Chem. Phys. **61**, 2478 (1974)
7. M.D. Di Rosa, R.K. Hanson, J. Quant. Spectrosc. Radiat. Transfer **52**, 515 (1994)
8. H. Trad, P. Higelin, N. Djebaili-Chaumeix, C. Mounaim-Rousselle, J. Quant. Spectrosc. Radiat. Transfer **90**, 275 (2005)
9. H. Okabe, *Photochemistry of Small Molecules* (Wiley, New York, 1978)
10. J. Mellqvist, A. Rosen, J. Quant. Spectrosc. Radiat. Transfer **56**, 209 (1996)

11. J. Luque, D.R. Crosley, *LIFBASE: Database and Simulation Program* (Version 1.6). SRI International Report MP 99-009 (1999)
12. R.J. Donovan, D. Hussain, L.J. Kirsch, Trans. Faraday Soc. **66**, 2551 (1970)
13. K.P. Huber, G. Herzberg, Constants of diatomic molecules (data prepared by J.W. Gallagher and R.D. Johnson, III), in *NIST Chemistry WebBook, NIST Standard Reference Database Number 69*, ed. by P.J. Linstrom, W.G. Mallard (National Institute of Standards and Technology, Gaithersburg, MD, 2005), http://webbook.nist.gov